

Conference paper

Chris William Anderson Bainbridge*, Chloe Eun Hye Lee, Neil Broderick and Jianyong Jin*

Mechanical modification of RAFT-based living polymer networks by photo-growth with crosslinker

<https://doi.org/10.1515/pac-2022-0803>

Abstract: In this work we present a study into the usage of crosslinker growth of Reversible addition-fragmentation chain-transfer polymerization (RAFT)-based Living Polymer Networks (LPNs) for the purpose of mechanical strengthening. Previous work with LPNs has thoroughly covered growth with monomers for various goals, and has touched on using a small amount of crosslinker during growth to retain mechanical strength after growth. Herein, we demonstrate growth with both purely crosslinker and purely monomer for the sake of comparison. We also show this across both symmetries of RAFT agent to see how their different growth behaviors affect the results. The asymmetric RAFT underwent a mesh-filling process during growth which resulted in both crosslinker and monomer strengthening the parent network to a similar degree. However, with the symmetric RAFT agent we saw that the crosslinker and monomer growth caused opposite effects due to their impact on the average crosslinking density; while monomer growth lowered it, growth with crosslinker increased it and strengthened the gel accordingly.

Keywords: Crosslinking; living polymer network; mechanical modification; POLY-CHAR; polymer characterization; RAFT.

Introduction

The most valuable property of living polymer networks (LPNs) is their ability to grow and morph from a parent network into a variety of daughter networks [1–7]. These can range from stimuli response and surface modification to mass growth and physical changes. In this work, we will focus primarily on physical modification and its effects on the mechanical properties of the network. The mechanical behavior of polymer networks is traditionally modified by the introduction of additives, or by branching into composite materials. One innovation unique to polymer networks was the creation of double networks (DNs) by Jian Ping Gong's research group [8–10]. These are a class of hydrogel characterized by a special network structure consisting of two polymer components with contrasting physical properties. This provides them with properties greater than either individually, as they contain both a rigid highly crosslinked network and a ductile loosely crosslinked network within the same macrostructure. They can be split further into two

Article note: A collection of invited papers based on presentations at the International Polymer Characterization Forum POLY-CHAR 2022, held as an online meeting based in Siegen (Germany), May 22–25 2022.

***Corresponding authors:** Chris William Anderson Bainbridge and Jianyong Jin, School of Chemical Sciences, The University of Auckland, Auckland 1010, New Zealand; and Dodd-Walls Centre for Quantum and Photonic Technologies, Auckland 1010, New Zealand, e-mail: e-mail: cbai804@aucklanduni.ac.nz (C.W.A. Bainbridge) and j.jin@auckland.ac.nz (J. Jin). <https://orcid.org/0000-0002-6135-3382> (C.W. A. Bainbridge), <https://orcid.org/0000-0002-5521-6277> (J. Jin)

Chloe Eun Hye Lee, School of Chemical Sciences, The University of Auckland, Auckland 1010, New Zealand; and Dodd-Walls Centre for Quantum and Photonic Technologies, Auckland 1010, New Zealand. <https://orcid.org/0000-0003-2671-3781>

Neil Broderick, Department of Physics, The University of Auckland, Auckland 1010, New Zealand; and Dodd-Walls Centre for Quantum and Photonic Technologies, Auckland 1010, New Zealand

groups: connected double networks (c-DNs) which contain some degree of inter-crosslinking between the two networks, and truly independent double networks (t-DNs) where the two components do not share any covalent bonds [8–10].

An alternative pathway in more recent years has been to leverage the living properties of LPNs to insert new blocks of polymer directly into the network. Among others, the Matyjaszewski group have demonstrated a great deal of post-production modification of LPNs through their work with structurally tailored and engineered macromolecular (STEM) networks [7, 11–14]. The first of the relevant STEM gel studies was in 2017, where they produced a network containing a radical inimer (initiating monomer), similar in form to the radical initiator Irgacure 2959, which upon activation with UV light would cleave to produce radicals and initiate a secondary polymerization [11]. In this case, the network was infiltrated with crosslinker to produce a densely crosslinked region semi-attached to the existing network when irradiated with UV light. Although growth with radicals in this manner is extremely fast, it is also uncontrolled and results in a messy network making further growth either difficult or impossible. While this is not technically an LPN, it is an earlier example which embodies what later work has gone on to achieve.

Further studies in 2018 saw the first use of atom transfer radical polymerization (ATRP) inimers to modify the networks by growing monomer chains in a controlled fashion [12]. The use of living polymerization techniques allows a greater amount of control over the growth, allowing it to be paused and continued at will. The networks were produced by a thermal Reversible addition-fragmentation chain-transfer polymerization (RAFT) polymerization of monomer, crosslinker, and ATRP inimer, which allowed the growth step to proceed by an orthogonal pathway to the formation, clearly distinguishing the two. Regions were controlled by a photomask and grown with photo-ATRP to be either hydrophobic or hydrophilic, depending on the inserted monomer. Temporal control was also used to adjust the extent of hydrophobic/philic behavior. Later work that year was focused on using these same STEM gels to produce soft elastomers [13]. Growth with butyl acrylate to produce soft chains was used to lower the compression modulus below that of the parent network. With sufficient growth, they were able to create supersoft networks with high resilience and withstand 100 % shear strain without permanent deformation.

2019 saw the switch to a fully RAFT-based system [14]. This approach used a regular RAFT agent and RAFT inimers that could be activated at different wavelengths. Under green light for formation, only the standard RAFT agent would induce polymerization, and the inimers could be inserted without activation. These parent networks could then be modified under blue light, activating both the regular RAFT and the inimers, to produce daughter networks with differing mechanical properties.

In 2017 the Johnson group performed a great deal of work into living polymer networks, which involved growth with a crosslinker and monomer mixture to produce daughter gels that could expand in size without sacrificing mechanical strength [15]. Typically, growth with a symmetric RAFT network results in a mesh-expansion process, lowering the average crosslinking density and making the daughter gel softer. They showed that with tuning, they were able to perform copolymer growth with a mixture of monomer and crosslinker such that the daughter gel's mechanical properties remained close to the parent gel despite increasing in both size and mass.

The main focus of this work will be demonstrating that we can sufficiently alter the mechanical properties of our one-pot LPNs [16] through post-production growth with a crosslinker. Our group has done some work previously using monomers for mechanical modification. However, growth purely with a crosslinker has not yet been demonstrated on an LPN. To show this, we grew samples in both monomer and crosslinker, to observe how the crosslinking interplays with the expected growth behavior of the different RAFT symmetries. We know from previous work [17] that the asymmetric RAFT follows a mesh-filling process during growth with monomer, resulting in increased density for the daughter gel. On the other hand, the symmetric RAFT agent undergoes mesh-expansion, which causes the opposite effect and results in the daughter gel becoming looser and showing an increased swelling ratio. We will start by exploring the mechanical modification through these behavioral mechanisms, and finish by looking at what happens when we perform further stages of growth with monomer and crosslinker to form successive granddaughter networks.

Experimental

Materials

All commercial monomers and solvents were purchased from Sigma Aldrich, used as received unless otherwise noted. These include; *N, N*-dimethylacrylamide (DMAM), poly (ethylene glycol) diacrylate (PEGDA) (average M_n 700), and 2-Hydroxyethyl acrylate (HEA). All monomers were filtered through basic alumina to remove inhibitors. 4-Cyano-4-[(dodecylsulfanylthiocarbonyl)sulfanyl]pentanoic acid (CDTPA) and 2,2'-[Carbonothioylbis(thio)]bis[2-methylpropanoic acid] (Diacid) were purchased from Boron Molecular, and used as received. All the other reagents were used as received unless otherwise specified.

Procedures

Formation of parent networks (LPN-A/S)

A typical experiment of a parent RAFT network formation was set up as follows: a glass vial was filled with HEA (284.5 μL , 2477.3 μmol), PEGDA 700 (387.1 μL , 619.3 μmol), CDTPA or Diacid RAFT (31.0 μmol), and DMSO (333.5 μL , 50 wt% monomers). The vial was sealed with a rubber septum and sparged with nitrogen for 10 min to remove any oxygen. The polymerization was carried under a blue LED light (460 nm, 0.7 mW/cm²) for 16 h to ensure high conversion. After polymerization the solid parent network was removed from the vial and washed in DMSO.

Growth of parent networks (LPN-A/S-M/XL)

A typical photo-growth for a parent network was carried out as follows: a growth medium containing either HEA (177.8 μL , 1548.3 μmol) or PEGDA 700 (967.8 μL , 1548.3 μmol), and DMSO which was added till the gel was submerged in the growth medium. The parent network was then soaked in this solution for 48 h, before being sealed with a rubber septum and sparged with nitrogen for 10 min to remove any oxygen. The vial was then irradiated under a green LED light (532 nm, 0.7 mW/cm²) for 48 h. After polymerization the daughter network was removed from the vial and washed in DMSO.

Growth of daughter networks (LPN-A/S-(XL-b-M))

A typical photo-growth for a daughter network was carried out as follows: a growth medium containing DMAM (153.5 μL , 1548.3 μmol) and DMSO, which was added till the gel was submerged in the growth medium. The parent network was then soaked in this solution for 48 h, before being sealed with a rubber septum and sparged with nitrogen for 10 min to remove any oxygen. The vial was then irradiated under a green LED light (532 nm, 0.7 mW/cm²) for 48 h. After polymerization the granddaughter network was removed from the vial and washed in DMSO.

Characterization

FTIR

Fourier Transform Infrared (FTIR) spectroscopy was used to observe evidence of successful growth through the differences in chemical composition. The model used was a Thermo Scientific Nicolet iS50 with attenuated total reflection (ATR) and a resolution setting of 4 cm⁻¹. Samples were washed consecutively in DMSO, MeCN, and THF before being thoroughly dried in a vacuum oven to ensure there was no solvent present during characterization.

Compression testing

Compression testing was used to measure the physical properties of our samples. We used an Instron 5567 with a 500 N load cell and a 30 mm diameter head. Measurements were performed at a constant rate of 1.00 mm/min until sample reached critical failure. The machine head was zeroed touching the top of the sample, and measurements of displacement and force were taken during operation. The samples were cylindrical in shape with approximate dimensions of 7.7–8.5 mm in height and 12.5–13.2 mm in diameter, variation in samples was due to differences in swelling ratios although exact measurements were taken and entered in the software prior to each test. The displacement and force were used to calculate the strain and compressive strength respectively. Parent samples were tested in triplicate for average values.

Results and discussions

Crosslinker growth of LPNs

We began by studying the absorbances of our chosen RAFT agents to see which wavelengths would be appropriate for formation and growth. Both CDTA (asymmetric) and the Diacid (symmetric) RAFT agents showed good absorbance in the blue (λ_{max} LED = 460 nm) range, and tailed into the green (λ_{max} LED = 532 nm) wavelength range enough to be useable (Fig. 2d). This allowed us to use blue light for formation, taking advantage of the greater kinetics and efficiency, while using green light for the growth to avoid polymerizing the crosslinker directly.

To produce the parent networks, we used an iniferter process under blue LED light (460 nm) in cylindrical vials sparged with nitrogen. PEGDA, HEA, and the RAFT agent were used in a 20:80:1 ratio, as samples with lower crosslinking took a very long time to reach gelation and would often form with physical imperfections and visual heterogeneity. The samples would then be carefully removed and swollen in a growth medium containing PEGDA or HEA and DMSO, before being grown under green LED light (532 nm) for a period of 48 h.

Figure 1 shows a cartoon which illustrates some of the possible differences between our asymmetric and symmetric networks, most importantly, the relative position of the RAFT trithiocarbonate groups within the wider mesh structure. LPN-A and LPN-S show the asymmetric and symmetric parent networks, respectively. Here we can see that the asymmetric RAFT positions itself as a living bud hanging off the otherwise dead mesh; in the growth stage this results in new chains threading in and around the existing structure, which remains unchanged. The symmetric RAFT is quite different in that it is positioned within the network chains, and during growth, it deforms the network as the new chains expand the original mesh structure. The next point to note is how these networks will change when grown with either monomer (LPN-A/S-M) or crosslinker (LPN-A/S-XL). Previous work shows that monomer growth on asymmetric and symmetric RAFT networks results in mesh-filling and mesh-expansion behavior, respectively [17]. We can reason from there that the asymmetric gels will become tougher as the network is filled up and becomes denser. Additionally, we can expect that crosslinker growth should cause a similar effect in filling up the interior volume of the network. However, with symmetric networks, we expect the opposite from monomer growth; they expand to increase the interior volume by lowering the average crosslinking density and, thus, getting softer. But if we picture this growth process with crosslinker we might expect the network to expand as with monomer growth. However, we can also expect densely crosslinked clusters to form around the RAFT agent which will act to increase the average crosslinking density and perhaps make it tougher instead of softer. There are some similarities in the LPN-A/S-XL samples to DN polymers, specifically with connected-DN (c-DN) examples. Unlike truly independent-DN (t-DN) polymers where the two networks are not chemically bound, c-DNs have some amount of inter-network crosslinking similar in a sense to LPNs grown with monomer and crosslinker. While the t-DN examples show better overall performance, the work with c-DNs demonstrates that having a second network, or pseudo-second network as with our grown LPNs, is an effective technique for increasing the toughness of gel samples (Table 1).

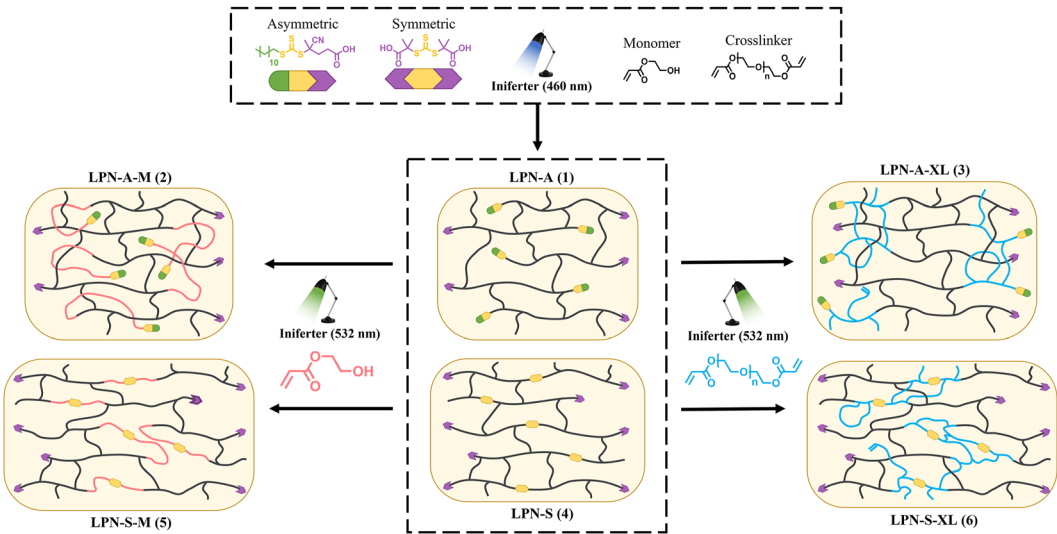


Fig. 1: Diagram showing the formation and subsequent growth of asymmetric (top row) and symmetric (bottom row) RAFT networks with monomer (left) and crosslinker (right). Samples were labelled as follows: LPN – [Symmetry of RAFT, A or S] – [Growth mixture, monomer (M) or crosslinker (XL). -b- used to denote blocks]. As such LPN-A-M denotes an asymmetric LPN grown with monomer.

Table 1: Table showing the compression modulus at 20 % strain, compression strength, and strain at break for the measured samples shown in Fig. 2. Brackets contain the average value for the three LPN parent samples.

Sample name	LPN-A	LPN-A-M	LPN-A-XL	LPN-S	LPN-S-M	LPN-S-XL
Compression modulus (MPa) at 20 % strain	3.029 (3.13 ± 0.35)	3.806	4.167	2.355 (2.34 ± 0.25)	1.896	4.703
Compression strength (kPa)	706 (723 ± 63)	1285	1354	656 (652 ± 38)	610	1169
Strain at break (%)	35.7 (35.5 ± 1.6)	38.9	40.2	35.1 (35.5 ± 1.5)	43.0	34.1

Starting with the asymmetric CDTPA samples, the first thing to note is that they look somewhat similar in their broad pattern. Considering the growth behavior which we discussed previously, this matches what we expected. Both crosslinker and monomer will be filling void space within the mesh much to the same result, which we can see in Fig. 2a where both reach similar stress and strain before failure. The LPN-A-M and LPN-A-XL both reach markedly higher final stress than their parent sample, almost doubling it from 706 kPa to ~1300 kPa. The final strain reached for both is also increased from the parent, but not to the same extent as the stress. Looking at the compression modulus, we can see that at 20 % strain both daughter samples have a higher gradient than the parent sample, with LPN-A-XL being slightly higher. It is clear then that the growth has achieved the desired effect of improving the mechanical properties of the parent network (LPN-A), increasing the compression strength and strain at break in both cases and thus, toughness. However, it is also worth noting that in the case of these asymmetric RAFT networks, growth with monomer is likely to be more desirable due to the wider variety and versatility of monomers available.

As we expected, the effects of growth on the symmetric Diacid samples are quite different. Here we can immediately see that the daughter samples have deviated and don't show the same similarity as the asymmetric samples (Fig. 2b). If we consider again the expected growth behavior for symmetric RAFT networks, they operate by a mesh-expansion mechanism where the chain in which the RAFT agent center is situated extends in

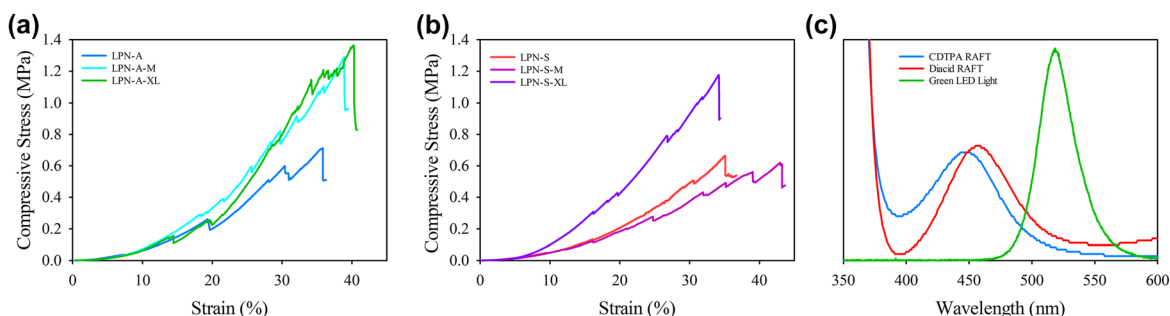


Fig. 2: Graphs showing the stress-strain plots from compression testing of the samples. (a) Asymmetric CDTA samples of 20 % crosslinked parent gel and daughter gels grown with either HEA or PEGDA. (b) Symmetric Diacid samples of 20 % crosslinked parent gel and daughter gels grown with either HEA or PEGDA. Small drops in stress prior to sample failure largely occurred due to the meniscus of the gel cracking off during the measurements. (c) Graph showing the overlap between the RAFT agent absorbance from UV-Vis and the green LED light emission spectra.

both directions. For growth with monomer this results in a decrease in the average crosslinking density depending on the extent of growth and the concentration of the RAFT agent; which in turn causes secondary effects such as an increased swelling ratio [15, 17]. However, if we consider growth with a crosslinker instead, we should expect an increase in the average crosslinking density by creating these comparatively dense blocks situated around the RAFT agent centers. Starting with LPN-S-XL, we can see that the compression strength has almost doubled from 656 kPa to 1169 kPa, while the strain has not shifted much. This shift was higher than expected given the comparatively low amount of crosslinker (50 DP) each RAFT agent was given to grow with, additionally with lower conversion due to steric restraint. The compression modulus at 20 % strain is also much higher than LPN-S, showing how the crosslinker growth has markedly improved the mechanical properties of the parent sample. LPN-S-M shows something entirely different. Here the compression strength has dropped slightly from 656 kPa to 610 kPa, but the sample was able to reach a higher strain before reaching the failure point. The compression modulus at 20 % strain is lower this time and shows how increasing the average mesh size loosens the network and it loses rigidity accordingly. This matches what we expected from the symmetric RAFT agent, wherein the monomer growth would decrease the average crosslinking density, and the crosslinker growth would increase it to soften and toughen the networks, respectively.

Multi-generational growth of LPNs

One of the well-known advantages of all controlled radical polymerization techniques is the ability to perform well-defined block polymerization. This has been thoroughly demonstrated with many forms of RAFT in linear systems. The benefit of block polymerization can be seen in its applications, notably with self-assembling nanomaterials such as polymerization-induced self-assembly (PISA) [18–21], and the increased effectiveness of responsive polymers [22–26]. However, for our work, we are simply interested in using it to show that we can shift the physical properties of our materials over consecutive generations of growth (Table 2).

We performed the multi-generational growth in the same manner as the crosslinker growth previously; the gels were swollen in the desired growth medium and then irradiated with green LED light (532 nm) to induce the iniferter polymerization process. Between the daughter and granddaughter growth stages, the samples were thoroughly washed several times with DMSO to ensure that none of the excess crosslinker would be inserted during the next growth step. The DMAM growth solution was given ~60 h to diffuse into the network, as drying the network would increase the chance of creating internal fractures, especially under a vacuum.

Table 2: Table showing the compression modulus at 20 % strain, compression strength, and strain at break for the measured samples shown in Fig. 3. Brackets contain the average value for the three LPN parent samples.

Sample name	LPN-S	LPN-S-XL	LPN-S-(XL _{PEGDA} -b-M _{DMAm})
Compression modulus (MPa) at 20 % strain	2.355 (2.34 ± 0.25)	4.866	3.724
Compression strength (kPa)	656 (652 ± 38)	1154	1244
Strain at break (%)	35.1 (35.5 ± 1.5)	36.5	42.2

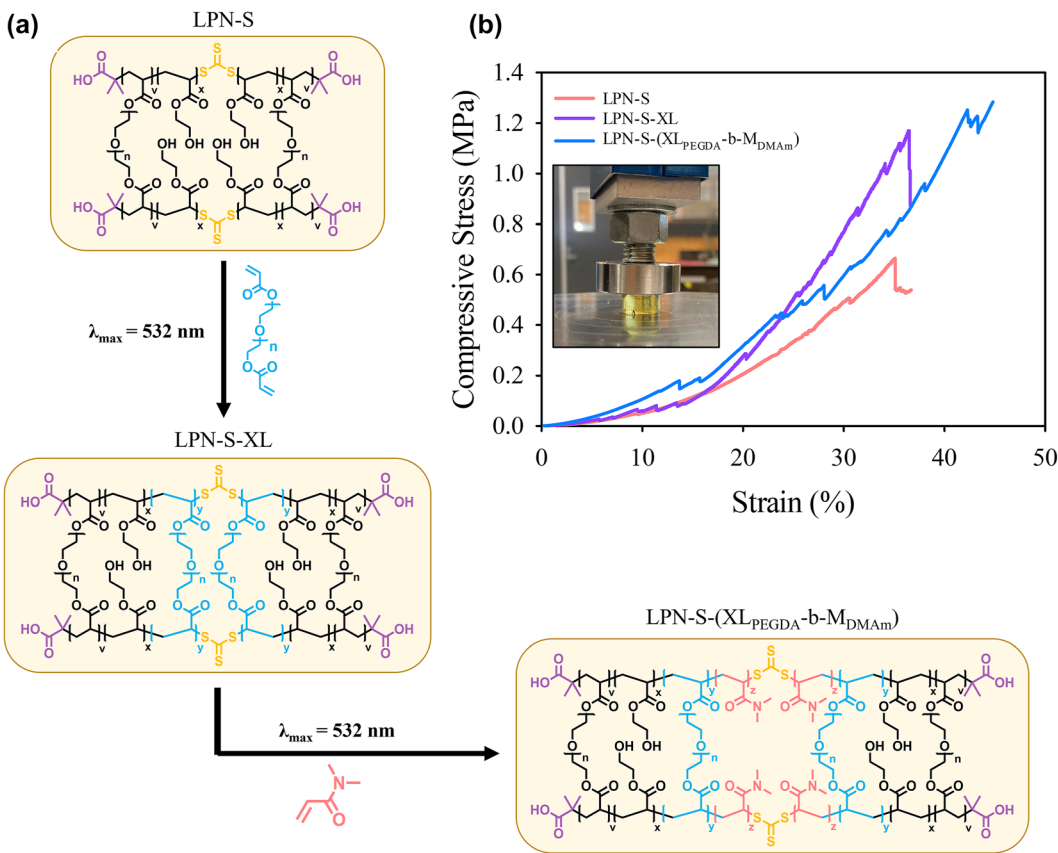


Fig. 3: Multi-generational growth of living polymer network (a) Diagram showing schemes for multi-generational growth of a symmetric RAFT network, first with the crosslinker PEGDA and subsequently the monomer DMAm. (b) Graph showing the stress-strain plots from compression testing of the parent, daughter, and granddaughter samples.

The parent and daughter samples follow similar trends to those discussed previously, with the daughter PEGDA grown sample (LPN-S-XL) showing increased compressive stress performance without the strain changing much. When we look at the results for the granddaughter sample (LPN-S-(XL-b-M)), we see the compression modulus has dropped beneath that of LPN-S-XL which has higher average crosslinking density, but is still higher than the original parent network; it has a similar compression strength to the crosslinker grown daughter network but with a noticeably improved strain prior to failure. Some of these improvements

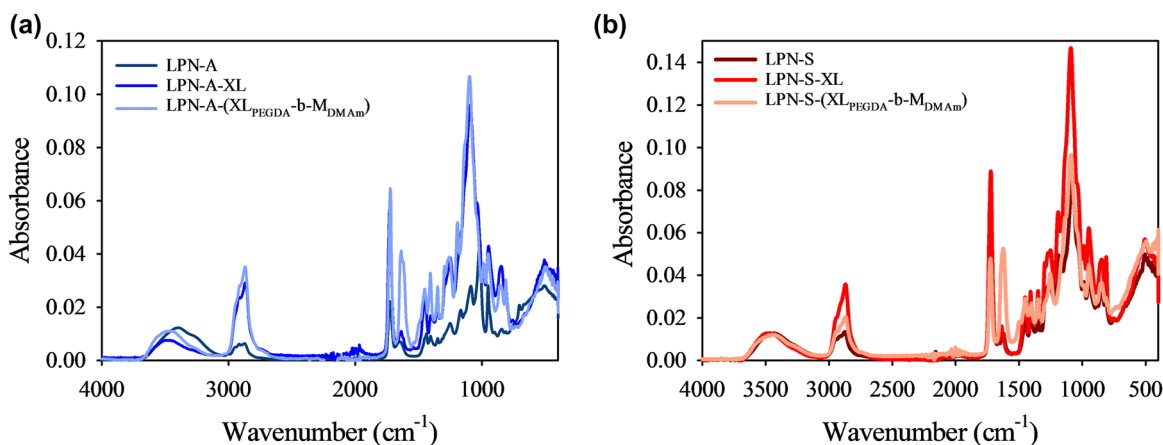


Fig. 4: Graphs showing the ATR FTIR absorbance plots for (a) CDTA samples at the parent (LPN-A), daughter (LPN-A-XL), and granddaughter (LPN-A-(XL-b-M)) stages. (b) Diacid samples at the parent (LPN-S), daughter (LPN-S-XL), and granddaughter (LPN-S-(XL-b-M)) stages.

may be due to the use of DMAM in place of HEA for the granddaughter growth stage, as DMAM has a higher glass transition temperature which would help toughen the network to some degree. If HEA had been used instead we have seen the granddaughter sample tend closer to the parent LPN-S, akin to Johnson *et al.* growing the gel in size whilst retaining overall physical properties [15].

To verify that the growth had indeed occurred, we took pieces of the gels (parent, daughter, and granddaughter), broken after compression testing, and thoroughly dried them out. This was done with one washing in DMSO, two washings in acetonitrile, and two washings in THF; before being dried in a vacuum oven overnight. These pieces were then analyzed using ATR FTIR to see if there were changes in the absorbance pattern after the insertion of crosslinker and monomer. As we can see in Fig. 4 the parent and daughter exhibit similar FTIR fingerprints; specifically around $\sim 3500\text{ cm}^{-1}$ we can see a substantial -OH peak arising primarily from HEA. Since the crosslinker PEGDA is present in the parent network we could not rely on observing different signals. Due to this we chose to use DMAM for growth of the daughter gel. In the granddaughter samples we can clearly see the amide C=O stretch at $\sim 1650\text{ cm}^{-1}$ on both plots, arising from the inserted DMAM monomer, meaning that it has been retained after thorough washing due to insertion into the network.

Conclusion

The purpose of this work was to study the effects of crosslinker growth as an option for post-production material modification of RAFT networks. We demonstrated that both asymmetric and symmetric RAFT networks could be grown with crosslinker to different effects. In the asymmetric samples, crosslinker growth achieved a similar effect to monomer growth, due to both undergoing mesh-filling behavior. With the symmetric RAFT samples we showed that while typical monomer growth would soften the sample, growth with crosslinker strengthened it by increasing the average crosslinking density. We then demonstrated further growth from parent – daughter – granddaughter to show how the properties could be tuned and adjusted. This serves as another step in the expanding capabilities of RAFT networks as a platform for performing a wide range of 4D modifications.

Research funding: J.J. N.B. and C.B. would like to thank the New Zealand Ministry of Business, Innovation and Employment (MBIE) Endeavour Fund for funding the Advanced Laser Microfabrication for NZ Industries Research Programme (Grant UOAX-1701).

References

- [1] J. Chiefari, Y. Chong, F. Ercole, J. Krstina, J. Jeffery, T. P. Le, R. T. Mayadunne, G. F. Meijs, C. L. Moad, G. Moad. *Macromolecules* **31** (16), 5559 (1998), <https://doi.org/10.1021/ma9804951>.
- [2] C. W. A. Bainbridge, A. Wangsadijaya, N. Broderick, J. Jin. *Polym. Chem.* **13** (11), 1484 (2022), <https://doi.org/10.1039/d1py01692j>.
- [3] M. Hartlieb. *Macromol. Rapid Commun.* **43** (1), 2100514 (2022), <https://doi.org/10.1002/marc.202100514>.
- [4] G. Opiyo, J. Jin. *Eur. Polym. J.* **159**, 110713 (2021), <https://doi.org/10.1016/j.eurpolymj.2021.110713>.
- [5] P. Pérez-Salinas, P. López-Domínguez, A. Rosas-Aburto, J. C. Hernández-Ortiz, E. Vivaldo-Lima. RAFT crosslinking polymerization. In *RAFT Polymerization: Methods, Synthesis and Applications*, Vol. 2, pp. 873–932 (2021).
- [6] S. Perrier. *Macromolecules* **50** (19), 7433 (2017), <https://doi.org/10.1021/acs.macromol.7b00767>.
- [7] J. Cuthbert, A. C. Balazs, T. Kowalewski, K. Matyjaszewski. *Trends Chem.* **2** (4), 341 (2020), <https://doi.org/10.1016/j.trechm.2020.02.002>.
- [8] J. P. Gong, Y. Katsuyama, T. Kurokawa, Y. Osada. *Adv. Mater.* **15** (14), 1155 (2003), <https://doi.org/10.1002/adma.200304907>.
- [9] J. P. Gong. *Soft Matter* **6** (12), 2583 (2010), <https://doi.org/10.1039/b924290b>.
- [10] M. A. Haque, T. Kurokawa, J. P. Gong. *Polymer* **53** (9), 1805 (2012), <https://doi.org/10.1016/j.polymer.2012.03.013>.
- [11] A. Beziau, A. Fortney, L. Fu, C. Nishiura, H. Wang, J. Cuthbert, E. Gottlieb, A. C. Balazs, T. Kowalewski, K. Matyjaszewski. *Polymer* **126**, 224 (2017), <https://doi.org/10.1016/j.polymer.2017.08.035>.
- [12] J. Cuthbert, A. Beziau, E. Gottlieb, L. Fu, R. Yuan, A. C. Balazs, T. Kowalewski, K. Matyjaszewski. *Macromolecules* **51** (10), 3808 (2018), <https://doi.org/10.1021/acs.macromol.8b00442>.
- [13] J. Cuthbert, T. Zhang, S. Biswas, M. Olszewski, S. Shanmugam, T. Fu, E. Gottlieb, T. Kowalewski, A. C. Balazs, K. Matyjaszewski. *Macromolecules* **51** (22), 9184 (2018), <https://doi.org/10.1021/acs.macromol.8b01880>.
- [14] S. Shanmugam, J. Cuthbert, J. Flum, M. Fantin, C. Boyer, T. Kowalewski, K. Matyjaszewski. *Polym. Chem.* **10** (19), 2477 (2019), <https://doi.org/10.1039/c9py00213h>.
- [15] M. Chen, Y. Gu, A. Singh, M. Zhong, A. M. Jordan, S. Biswas, L. T. Korley, A. C. Balazs, J. A. Johnson. *ACS Cent. Sci.* **3** (2), 124 (2017), <https://doi.org/10.1021/acscentsci.6b00335>.
- [16] A. Bagheri, C. Bainbridge, J. Jin. *ACS Appl. Polym. Mater.* **1** (7), 1896 (2019), <https://doi.org/10.1021/acsapm.9b00458>.
- [17] C. W. A. Bainbridge, N. Broderick, J. Jin. *Polym. Chem.* **12** (35), 5017 (2021), <https://doi.org/10.1039/d1py00796c>.
- [18] S. L. Canning, G. N. Smith, S. P. Armes. *Macromolecules* **49** (6), 1985 (2016), <https://doi.org/10.1021/acs.macromol.5b02602>.
- [19] K. Ren, J. Perez-Mercader. *Polym. Chem.* **8** (23), 3548 (2017), <https://doi.org/10.1039/c7py00558j>.
- [20] M. Morimura, S. Ida, M. Oyama, H. Takeshita, S. Kanaoka. *Macromolecules* **54** (4), 1732 (2021), <https://doi.org/10.1021/acs.macromol.0c02569>.
- [21] J. Wan, B. Fan, S. Thang. *Chem. Sci.* **13**, 4192 (2022), <https://doi.org/10.1039/d2sc00762b>.
- [22] S. Dutta, D. Dhara. *J. Appl. Polym. Sci.* **132** (44), Article 42749 (2015), <https://doi.org/10.1002/app.42749>.
- [23] Q. Liu, P. Zhang, A. Qing, Y. Lan, M. Lu. *Polymer* **47** (7), 2330 (2006), <https://doi.org/10.1016/j.polymer.2006.02.006>.
- [24] Q. Liu, P. Zhang, A. Qing, Y. Lan, J. Shi, M. Lu. *Polymer* **47** (20), 6963 (2006), <https://doi.org/10.1016/j.polymer.2006.08.009>.
- [25] A. B. Lowe, M. Torres, R. Wang. *J. Polym. Sci. Polym. Chem.* **45** (24), 5864 (2007), <https://doi.org/10.1002/pola.22338>.
- [26] T. Tang, V. Castelletto, P. Parras, I. W. Hamley, S. M. King, D. Roy, S. Perrier, R. Hoogenboom, U. S. Schubert. *Macromol. Chem. Phys.* **207** (19), 1718 (2006), <https://doi.org/10.1002/macp.200600309>.